

NMR in high-pressure phases of solid NH_3 and ND_3

Montee A. Doverspike, Shang-Bin Liu, Pat Ennis, Tim Johnson, and Mark S. Conradi
Department of Physics, College of William and Mary, Williamsburg, Virginia 23185

K. Luszczynski and R. E. Norberg
Department of Physics, Washington University, St. Louis, Missouri 63130
 (Received 17 July 1985)

Pulsed NMR experiments have been performed under pressure ($P < 4.1$ kbar) on phases I and II of solid NH_3 and ND_3 . Line narrowing in NH_3 -II demonstrates that rapid rotations and diffusion occur. The proton T_1 reflects an activation energy of diffusion of 4400 K ($\pm 20\%$). The jump time close to the melting point in NH_3 -II is 6×10^{-8} s. The hexagonal structure of ND_3 -II is confirmed by the observation of a small quadrupole splitting of the deuteron spectrum. The orientation correlation time, as determined from the deuteron T_1 , is 1.0×10^{-12} s. Thus, ammonia-II is a typical rotor-phase solid. In NH_3 -I, the pressure dependences of the proton T_1 and T_{1D} are used to determine the activation volumes of threefold rotations and diffusion, respectively. By comparing with stimulated-echo experiments in ND_3 -I, we find a small isotope effect upon the diffusion rate. No proton or deuteron NMR evidence was found corresponding to the previously reported premelting transition indicated by the anomalous attenuation of ultrasound in phase I.

INTRODUCTION

There has been much interest recently in the condensed phases of ammonia under high pressures.¹⁻⁵ Besides the phase (NH_3 -I) stable at low pressures, three new phases have been found along the melting curve.²⁻⁵ An unusual, critical-like increase in the compressibility of the solid near the melting transition has been observed.¹ Because NH_3 forms hydrogen bonds between the molecules, some of the interest in ammonia stems from its similarity to water.

The phase diagram of NH_3 is shown in Fig. 1, taken from Refs. 2 and 3. At lower temperatures than are shown in that diagram, NH_3 -I is the stable phase. Phase I is an orientationally ordered cubic structure with space

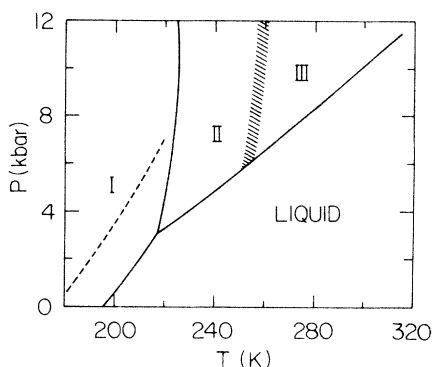


FIG. 1. From Fig. 2 of Ref. 2 and Fig. 2 of Ref. 3; phase diagram of ammonia near the melting curve. At lower temperatures, phase I is stable. The II-III transition appears broad because it is sluggish. The dashed curve shows the location of the ultrasonic attenuation anomaly. That is, to higher temperatures, ultrasound is heavily attenuated; to lower temperatures, ultrasound propagates readily.

group $P2_13$.^{6,7} This consists of four interpenetrating sublattices, each simple cubic, with the molecular centers of gravity displaced from face-center locations. All of the molecules on any one sublattice are oriented parallel, with the molecule's threefold axis along one of the body diagonals of the cube. This structure allows a given NH_3 molecule to participate in six hydrogen bonds: three involve the given molecule's nitrogen with hydrogens from other molecules and the other three involve each of the given molecule's hydrogens with the nitrogen atoms of three other molecules.⁷

In phase I, NH_3 molecules undergo thermally activated threefold reorientation as seen by NMR.^{8,9} At the melt the rate of reorientations⁸ is $\sim 10^{10} \text{ s}^{-1}$. At low temperatures, the proton NMR linewidth does not rise to its predicted rigid-lattice value due to the threefold quantum tunneling.⁸ It should be noted that these reorientations require the breaking and reforming of hydrogen bonds. Slow diffusion has been observed in NH_3 -I, the jump rate reaching $3 \times 10^4 \text{ s}^{-1}$ at the melt at zero pressure.¹⁰

During an investigation of the phase diagram of solid NH_3 , Mills and co-workers found that 10- and 30-MHz ultrasound echoes became undetectably small in phase I along the dashed curve in Fig. 1.² That is, to the left of the curve strong ultrasound echoes were obtained, but to the right no echoes were received. The transition was quite sharp; the location of the transition was reproduced during heating, cooling, increasing pressure, and decreasing pressure. This behavior is too sudden to be a relaxation effect; rather, a subtle phase transition is suggested. One of the goals of this work was to seek NMR evidence for the nature of the changes in NH_3 -I at the ultrasonic anomaly.

Solid phase II of ammonia is stable only near the melting curve. Neutron diffraction⁴ indicates that the structure is orientationally disordered hcp with space group

$P6_3/mmc$, the same structure as β -N₂.¹¹ Together these facts suggest that NH₃-II is a rotor ("plastic") crystal. No ultrasound echoes were observed² in this phase, presumably reflecting a high attenuation—common in rotor solids.¹² Thus, a second goal of the present work was to determine whether NH₃-II is indeed a rotor solid. If so, we sought to compare the behavior of NH₃ with more "normal" rotor solids: the hydrogen bonding in NH₃ suggests that it may be an unusual rotor crystal.

The maximum pressure available to us (4.1 kbar) precluded any study of phases III (Fig. 1) or IV at still higher pressures,^{4,5} not shown in Fig. 1.

EXPERIMENTAL DETAILS

The ammonia sample was compressed hydrostatically by helium gas. Helium gas at tank pressure (160 bars) was passed through a liquid-nitrogen trap to remove water, a particle filter, and an O₂ getter (to avoid putting paramagnetic O₂ into the sample). The helium was compressed to 2 kbar (1 bar = 10⁵ N/m²; 1.013 bar = 1 atm = 14.7 psia) in a reciprocating-diaphragm compressor (Aminco, now Newport Scientific, Jessup, MD). To reach higher pressures a cryogenic intensifier was used. This was a beryllium copper cylinder (alloy 25 from Cabot Corp., Reading, PA) 12 in. long, 1 in. o.d., and with a $\frac{1}{4}$ -in. bore. While immersed in liquid nitrogen it was filled with He at 2 kbar. The diaphragm unit was then valved-off and the intensifier placed in a room-temperature explosion shield; the pressure rose to 4 kbar as the intensifier warmed. A fine adjustment of the pressure was accomplished by putting the intensifier in warm water. Though this method of pressurization is crude, it is simple and involves only one valve and no sliding seals. The high pressure was measured with a Manganin resistance gauge of our design which was calibrated against a Heise (Bourdon-tube) gauge. Whenever possible we used narrow bore tubing (0.006 in. i.d.); this kept the dead volume small and increased the time constant of the system, decreasing the hazard of explosions.

The NH₃ gas was purchased from Matheson (anhydrous grade) and the ND₃ was obtained from Merck (99.5 at. % D). The samples were condensed as liquids into the sample cell with a chloroform liquid-solid slush cooling the cell to 210 K. The sample cell was then cooled in liquid nitrogen; helium gas was added at 160 bars to prevent the now solid sample from later moving out of the cell by sublimation and/or condensation. The sample cell was then put into the thermostatted, flowing-N₂-gas stream of our gas-flow research Dewar. The temperature was measured with a platinum-resistance thermometer and a copper-Constantan thermocouple, both located just above the sample cell. The temperatures reported are precise to ± 0.2 K and accurate to ± 1 K.

The sample cell was made of titanium alloy (6 at. % Al, 4 at. % V; from Tico, Farmington Hills, MI). Titanium was used because it does not react with ammonia; we feared that even slow corrosion of beryllium copper could weaken such a cell. The cell had a 0.68 in. o.d. and the inner diameter was 0.16 in. The cell was sealed with a brute-force conical plug, as was the intensifier. The NMR

coil, 0.1 in. in diameter and 0.5 in. long, resided in the cell and was centered by a thin Teflon tube. The coil was grounded on one end; the other end ran up the sample-helium fill tube to room temperature. A thermocouple feedthrough (sealed with a drop of oil instead of epoxy) was used to take the wire to room pressure.¹³

We noticed that the T_1 of liquid NH₃ condensed into the titanium cell was only about 1 s, shorter than the 8 s reported previously.⁹ This is probably due to paramagnetic ions present from chemical attack by the NH₃. To ensure that dissolved O₂ was not the cause, we condensed some of the same NH₃ into a Pyrex tube. The T_1 of this sample agreed with the literature value.

We remark that our low-pressure gas-handling apparatus used copper tubing and brass valves. Dry ammonia did not attack the system to any observable extent. The NMR apparatus has been described previously.¹⁴

Our cell design has a region of strong rf electric field between the coil and the cell wall. This electric field evidently coupled to the piezoelectricity of ammonia in phase I. Immediately after transmitter pulses an intense transient signal was observed in the receiver. This transient was present even without the dc magnetic field, so NMR and acoustic ringing are ruled out. The transient disappeared in liquid ammonia and in phase II; thus, the transient is from the piezoelectricity of phase I. At low pressures this signal was often much larger than the NMR signal. The piezoelectric transient became small at high pressures and at high resonance frequencies. The amplitude of the piezoelectric transient from ND₃-I did not change upon passing through the dashed curve of Fig. 1 at 4.0 kbar. It is not known whether the ultrasound propagated primarily through the ammonia or the titanium cell. The NMR signal of phase I was always observed using add-and-subtract averaging techniques that relied on the inversion of spin-resonance signals. That is, a blinking 180° pulse (blinked off every other time) preceded each pulse sequence; thus the piezoelectric transient was canceled.

PHASE II: RESULTS AND DISCUSSION

The proton T_1 and T_2 for NH₃-II are reported in Fig. 2. The T_2 data were obtained from free-induction decays (FID's) and may suffer slightly from magnetic field inhomogeneity. The data were taken at a pressure of 4.0 kbar, essentially the highest pressure available to us. Hence, only a 10-K "window" of phase II could be studied (see phase diagram, Fig. 1).

The long T_2 values, of order 1 ms, demonstrate that both molecular rotations and translational diffusion narrow the NH₃-II proton line. Both the intramolecular and intermolecular proton-proton dipolar couplings are averaged to nearly zero. For example, if only isotropic molecular rotations occurred, the second moment (M_2) of the resonance would be 5.0×10^9 rad²/s² (see below). This would correspond to a T_2 of approximately $M_2^{-1/2}$, or 14 μ s. The line narrowing from rotations and diffusion demonstrates that NH₃-II is indeed a rotor (plastic) crystal. Although the proton T_2 indicates the existence of both rotations and diffusion, the ¹⁴N-proton indirect

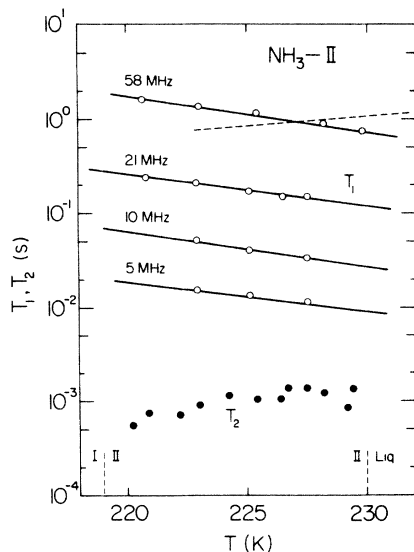


FIG. 2. Proton T_1 (open circles) and T_2 (solid circles) in $\text{NH}_3\text{-II}$ at 4.0 kbar. T_1 was measured at several frequencies; the nearly ω_{NMR}^2 dependence of T_1 indicates that the diffusion jump rate ω_j is slower than ω_{NMR} . The solid lines which are fit to the proton T_1 correspond to an activation energy of 4400 K. The long T_2 values increase with temperature due to motional narrowing. The dashed curve shows the deuteron T_1 data at 8.9 MHz; data points are omitted to avoid confusion.

("J") spin coupling will interfere with any quantitative analysis of T_2 .⁹ The indirect interaction is modulated by chemical exchange; this is readily catalyzed in ammonia by traces of water.

The proton spin-lattice-relaxation times T_1 in Fig. 2 decrease with temperature and display a strong frequency dependence: $T_1 \propto \omega_{\text{NMR}}^2$. This is exactly what is expected for relaxation due to slow motions. For a motion of correlation time τ_j with $\omega_{\text{NMR}}\tau_j \gg 1$,¹⁵

$$1/T_1 = 2.29M_2/\omega_{\text{NMR}}^2\tau_j. \quad (1)$$

Here, M_2 is the second moment (mean square) of the spin interactions modulated by the motion. The above equation predicts $T_1 \propto \omega_{\text{NMR}}^2$ and, because τ_j decreases with temperature for thermally activated motions, T_1 decreases with temperature. Given that the motion responsible for spin-lattice relaxation is slow ($\tau_j > \omega_{\text{NMR}}^{-1} \approx 10^{-8}$ s), this motion must be molecular jump diffusion. This is confirmed by our deuteron T_1 measurements in $\text{ND}_3\text{-II}$ which find very rapid reorientations (see below).

Because τ_j and T_1 in Eq. (1) are directly proportional, the temperature dependence of T_1 was used to deduce the activation energy of diffusion in $\text{NH}_3\text{-II}$. The result is $E/k = 4400$ K ($\pm 20\%$); the large uncertainty is due to the small temperature interval of phase II. The solid lines in Fig. 2 have slopes corresponding to this activation energy.

Boden considers several scaling relations for the activation energy of diffusion in rotor crystals.¹⁵ One of these is due to van Liempot,¹⁶

$$E/kT_m = \text{const},$$

where T_m is the melting temperature. For a great variety of rotor (plastic) crystals,¹⁵ the constant is 22 ± 4 . The value of this ratio in ammonia is 19, using the above activation energy and the melting temperature along the 4.0-kbar isobar.² Thus, translational diffusion in $\text{NH}_3\text{-II}$ is well described by the scaling relation.

The correlation time τ_j for jump diffusion may be obtained from Eq. (1) and the T_1 data, if M_2 is known. We assume that the intramolecular dipole-dipole interactions are averaged to zero by molecular rotation; this is a good approximation, as indicated from the $\text{ND}_3\text{-II}$ results (see below). The remaining intermolecular M_2 may be computed readily if one assumes uncorrelated and isotropic rotations.¹⁷ In that case, all three protons may be "placed" at the molecular center (the ^{14}N contribution is trivial) and the Van Vleck second moment computed.¹⁸ The result in $\text{NH}_3\text{-II}$ is $M_2 = 5.0 \times 10^9 \text{ rad}^2/\text{s}^2$. This M_2 is used in Eq. (1) along with high-frequency data (so that $\omega_{\text{NMR}}\tau_j \gg 1$ is well satisfied); at the melt τ_j is 6×10^{-8} s.

We have also determined τ_j from the frequency dependence of T_1 at a fixed temperature of 225 K. Whereas at high frequencies $T_1 \propto \omega_{\text{NMR}}^2$, the dependence becomes weaker as $\tau_j\omega_{\text{NMR}}$ approaches 1. Using the calculations of Resing and Torrey,¹⁹ the best fit to the data was obtained with $\tau_j = 7 \times 10^{-8}$ s ($\pm 25\%$). This value may be used to predict a value of $\tau_j = 4.5 \times 10^{-8}$ s at the melt (230 K) using the above-determined activation energy. The two determinations of τ_j at the melt are in good agreement. It should be noted that other calculations¹⁵ of T_1 yield numerically different values in Eq. (1) and have slightly different frequency dependences near the condition $\tau_j\omega_{\text{NMR}} = 1$. Thus, the τ_j values determined here are model sensitive and are probably accurate only to within a factor of 2.

The value of τ_j at the melting point in rotor solids is typically¹⁵ 10^{-6} to 10^{-7} s. Thus, the rate of diffusion in $\text{NH}_3\text{-II}$ at the melt is within a factor of 2 of the band of typical values.

The rotational behavior of ammonia molecules in phase II is revealed by the deuteron resonance of $\text{ND}_3\text{-II}$. The principal spin interaction is between the quadrupole moment of the nucleus and the electric field gradient (EFG) from the bonding electrons. The spectra of two samples of $\text{ND}_3\text{-II}$ at 4.0 kbar are shown in Fig. 3. Each spectrum consists of several doublets ($m_1 = -1 \rightarrow 0$ and $0 \rightarrow 1$), indicating that several crystallites are present. The small size of the splittings (500 Hz), when compared to the strength of the quadrupolar interaction [245 kHz (Ref. 20)], indicates a great deal of motional averaging due to rotations.

In greater detail, the EFG at a deuteron is approximately uniaxially symmetric along the N—D bond. Threefold reorientations about the molecular threefold axis will produce a time-average EFG with uniaxial symmetry along the threefold axis.¹⁸ The strength of the interaction is now reduced by the factor $\frac{3}{2}\cos^2\alpha - \frac{1}{2}$, where α is the angle between the N—D bond and the threefold axis. For nearly tetrahedral geometry of ND_3 ,^{6,7} this factor is $-\frac{1}{3}$. In phase II the threefold axis rotates as well, producing further motional averaging. Because the hcp structure of $\text{ND}_3\text{-II}$ (determined from neutron diffraction⁴) has one

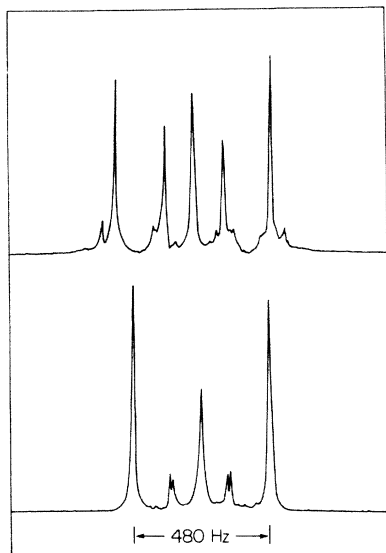


FIG. 3. Quadrupole-split deuteron spectra of two samples of ND₃-II at 8.9 MHz. The many doublets correspond to crystallites with different orientations relative to the magnetic field. The small size of the splittings demonstrates a nearly isotropic molecular orientation probability distribution in the hexagonal structure of phase II.

unique axis (the *c* axis) and higher than twofold symmetry about the *c* axis, it can be shown using the addition theorem of spherical harmonics,^{18,21,22}

$$\Delta f = \frac{3}{2} [e^2 q Q / h] \left(\frac{3}{2} \cos^2 \alpha - \frac{1}{2} \right) \times \left\langle \left(\frac{3}{2} \cos^2 \theta - \frac{1}{2} \right) \left(\frac{3}{2} \cos^2 \psi - \frac{1}{2} \right) \right\rangle. \quad (2)$$

Here, Δf is the quadrupole splitting, θ is the instantaneous angle between the threefold axis and the *c* axis, and ψ is the angle between the *c* axis and the dc magnetic field. The term in square brackets is 245 kHz.²⁰

We assume that one of the crystallites in Fig. 3 had an orientation near $\psi=0$. Thus, since the maximum splitting is about 500 Hz, we have

$$\left\langle \frac{3}{2} \cos^2 \theta - \frac{1}{2} \right\rangle = \pm 4 \times 10^{-3}.$$

If none of the crystallites were at $\psi=0$, the above value underestimates the true $\langle \frac{3}{2} \cos^2 \theta - \frac{1}{2} \rangle$. In any event, $\langle \frac{3}{2} \cos^2 \theta - \frac{1}{2} \rangle$ is a measure of the $l=2$ deviation from sphericity of the orientational probability distribution. Because the deviation is so small, the orientations appear to be isotropic. We note that there may be larger deviations from isotropy for $l>2$, but NMR cannot detect these.

Because of the rapid diffusion in phase II, it may be assumed the molecules sample all equivalent sites in NMR timescales (10^{-5} s). In this case, the time-average EFG must be zero in a perfect cubic crystal.¹⁸ Thus, the existence of the splitting confirms the non-cubic structure of phase II. β -N₂ and β -CO are both rotor solids with hcp structure (space group¹¹ $P6_3/mmc$ for β -N₂); most other rotor solids are fcc or bcc. In β -N₂ (Ref. 21) and β -CO

(Ref. 23) the value of $|\langle \frac{3}{2} \cos^2 \theta - \frac{1}{2} \rangle|$ is about 1×10^{-3} . Hence, when compared to other rotor solids of hcp structure, ND₃-II seems a typical rotor crystal.

The deuteron spin-lattice relaxation in ND₃-II is from rotations modulating the quadrupole interactions. Because M_2 in Eq. (1) scales²⁴ with $I(I+1)\gamma^4$, where γ is the magnetogyric ratio, the translational diffusion alone would yield a deuteron T_1 of 15 s at 8.9 MHz. Since the observed T_1 (Fig. 2) is much smaller and has the opposite temperature dependence compared to the proton T_1 , diffusion is not the source of spin-lattice relaxation in ND₃-II. For isotropic reorientations and a uniaxially symmetric EFG, and with $\omega_{\text{NMR}}\tau_r \ll 1$,^{15,24}

$$T_1^{-1} = \frac{3}{8} [e^2 q Q / \hbar]^2 \tau_r. \quad (3)$$

Here, τ_r is the orientation correlation time for $l=2$ functions of orientation and the term in square brackets is $2\pi \times 245$ kHz. The observed T_1 of 1.1 s near the melt yields $\tau_r = 1.0 \times 10^{-12}$ s. This value is typical of rotor solids.¹⁵

We note that the assumption of isotropic reorientations may not be correct—rotations of and about the threefold axis are different. If one assumed infinitely rapid threefold reorientations, Eq. (3) would predict $\tau_r = 9 \times 10^{-12}$ s for reorientations of the threefold axis. However, this model seems unphysical. In either case, the motions satisfy $\tau_r \omega_{\text{NMR}} \ll 1$.

The value of $\tau_r = 1.0 \times 10^{-12}$ s may be compared to the inertial limit. Steele²⁵ has shown that for $l=2$ functions of spherical free rotors, using a Gaussian approximation to the correlation function,

$$\tau_r = 0.51 (I/kT)^{1/2}. \quad (4)$$

For ND₃ we have used the above relation with the average of the three principal values of inertia. The result is $\tau_r = 0.074 \times 10^{-12}$ s. Of course, the exact value will be slightly different because ND₃ is a symmetric top. Nevertheless, the observed τ_r is about 14 times longer than the inertial limit. In many organic rotor solids, τ_r at the melting point is within a factor of 2 of the inertial limit.¹⁵

We had expected that the hydrogen bonding in ammonia would make phase II an unusual rotor solid. For example, τ_r is very long in cyclohexanol¹⁴ (10^{-9} s) and pivalic acid¹⁵ (2×10^{-10} s) at the melting point. However, ammonia phase II appears to be an ordinary rotor solid: its diffusion rate at the melt, diffusion activation energy, and nearly isotropic orientation distribution are all rather typical. The only unusual aspect is that its orientation correlation time is substantially longer than the inertial limit.

PHASE I: RESULTS AND DISCUSSION

Phase I of solid NH₃ is orientationally ordered.^{6,7} Two kinds of thermally activated motions occur in phase I, as observed previously with proton NMR.⁸⁻¹⁰ First, threefold reorientations of the molecules occur about the threefold molecular axes. The rate of threefold reorientations can be determined from the proton T_1 .^{8,9} The second kind of motion is diffusion; in the orientationally ordered

structure, reorientation must accompany translational diffusion. The diffusion dominates the low-field spin-relaxation times $T_{1\rho}$ (rotating-frame longitudinal relaxation¹⁰) and T_{1D} (relaxation of dipolar order).

We have measured the proton T_1 and T_{1D} of $\text{NH}_3\text{-I}$ at three pressures; the results appear in Fig. 4. The zero-pressure data in Fig. 4 are generally in agreement with previous work.⁸⁻¹⁰ Because T_1 increases with temperature, the rate ω_3 of threefold reorientations is greater than the resonance frequency (58.4 MHz). Hence, $T_1 \propto \omega_3$ and the temperature dependence of T_1 may be used to determine the activation energy of threefold reorientations. The results are listed in Table I; the zero-pressure values agree with the two previous determinations.

The pressure dependences of T_1 and ω_3 may be interpreted in terms of activation volumes. It is standard to write²⁶

$$\omega = \omega'_0 e^{-\Delta E/kT} e^{-P\Delta V/kT} \quad (5)$$

ΔE and ΔV are taken to be constant, and are the activation energy and volume, respectively. The constant ω'_0 includes any entropic terms and the attempt frequency. We have plotted T_1 on a logarithmic scale as a function of pressure along the $T=160$ K and $T=190$ K isotherms. From the slopes of the straight lines obtained, $\Delta V=1.9$ cm^3/mol at 160 K and 2.4 cm^3/mol at 190 K. Hence, given the small pressure dependence of T_1 (only 50% change for 4 kbar), ΔV is 2 cm^3/mol ($\pm 25\%$). The molar volume V_m of $\text{NH}_3\text{-I}$ is approximately 20.45 cm^3 ;⁶ hence, ΔV for the threefold reorientation is 0.1 V_m .

The reduced activation volume of 0.1 (ratio of activation volume to molecular volume) may be compared to

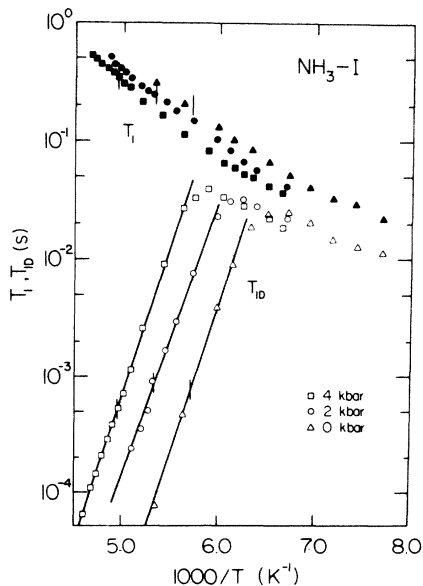


FIG. 4. Proton T_1 (solid symbols) and T_{1D} (open symbols) from $\text{NH}_3\text{-I}$ at three pressures. Threefold reorientations determine T_1 . Jump diffusion determines T_{1D} at high temperatures; at lower temperatures T_{1D} is limited by T_1 processes. The solid lines correspond to thermally activated jump diffusion with parameters listed in Table I. The short lines cross the data at the temperatures of anomalous ultrasonic attenuation.

that of benzene. In benzene, an orientationally ordered solid, sixfold reorientations of the planar molecule occur. The reduced activation volume is 0.18 according to one study²⁷ and 0.07 according to another.²⁸ Our value for $\text{NH}_3\text{-I}$ is reasonable, by comparison. It should be noted that in several rotor (plastic) organic crystals²⁶ the reduced activation volumes for rotation are between 0.04 and 0.09.

We note that all the activation energies E in Table I are measures of the temperature dependences along isobars. That is, they correspond to the equation

$$\omega = \omega_0 e^{-E/kT} \quad (6)$$

where ω_0 and E are functions of the pressure. The frequencies and energies in Eqs. (5) and (6) are related but not equal.

Also shown in Fig. 4 are our results for T_{1D} in $\text{NH}_3\text{-I}$ at three pressures. T_{1D} is the relaxation-time constant for nuclear-spin dipolar order^{18,29,30} (order in which spins are preferentially aligned along their local fields). T_{1D} was measured using the Jeener-Broekaert pulse sequence. At high temperatures, T_{1D} is determined by the rate ω_j of jump diffusion. According to the theory of relaxation by ultraslow motions,^{18,29,30}

$$T_{1D}^{-1} = \omega_j 2(1-p) \quad (7)$$

where p measures the extent of site-to-site correlation of the local fields. The product $2(1-p)$ is essentially unity.^{31,32} Assuming that $2(1-p)=1$, T_{1D} becomes equal to $\tau_j \equiv \omega_j^{-1}$, the mean jump time.

At each pressure the T_{1D} data have been analyzed using Eq. (6); the activation energies E and the prefactors ω_0 appear in Table I. At zero pressure, both the activation energy and prefactor from this work are higher than those reported earlier by O'Reilly and Peterson.¹⁰ The measured values of ω_j from this work and Ref. 10 are in reasonable agreement near 190 K, but the slopes of the data are different. We do not at present understand this difference in slopes. The results of the present work will be used in the following discussion, because the T_{1D} experiment is more straightforward to perform and interpret than the $T_{1\rho}$ experiment (for example, see Refs. 9 and 10).

The prefactor frequency ω_0 in Table I from Eq. (6) is much larger than typical lattice frequencies. Similar high values have been observed in the orientationally ordered solids $\alpha\text{-CO}$,³³ CO_2 ,³⁴ N_2O ,³⁵ and benzene.^{36,37}

The activation energy for diffusion at zero pressure listed in Table I and obtained from Eq. (6) may be compared to the latent heat of sublimation L_s at the triple point (gas-liquid-solid I). Taking 29.01 kJ/mol as L_s ,³⁸ the ratio E/L_s is 1.68. This is much lower than the values found in $\alpha\text{-CO}$,³³ CO_2 ,³⁴ N_2O ,³⁵ and benzene,^{36,37} all of which are 2.15 ± 0.03 . Presumably, this exception to simple scaling reflects that $\text{NH}_3\text{-I}$ is not a van der Waals solid, but has important hydrogen bonding.

The pressure dependence of T_{1D} in $\text{NH}_3\text{-I}$ may be interpreted as a volume of activation using Eq. (5); we find $\Delta V = 16 \pm 1$ cm^3/mol . Thus ΔV is 0.78 ± 0.05 molecular volume. Since ΔV is nearly one molecular volume, it is reasonable to assume a monovacancy mechanism for diffusion in $\text{NH}_3\text{-I}$. The reduced activation volumes for a

TABLE I. Activation energies and rate prefactors for motions in NH₃-I.

	$P=0$	$P=2.0$ kbar	$P=4.0$ kbar
E/k for threefold reorientations, from proton T_1 ; in K	1280 1160 ^a 1210 ^b	1390	1520
E/k for diffusion, from proton T_{1D} ; in K	5870 4730 ^c	5990	5940
ω_0 prefactor for diffusion (s ⁻¹)	5.0×10^{17} 1.0×10^{15} ^c	1.0×10^{17}	1.2×10^{16}

^aFrom Ref. 8.^bFrom Ref. 9.^cFrom Ref. 10, $T_{1\rho}$ measurements.

number of organic rotor (plastic) crystals²⁶ range between 0.57 and 1.2; for benzene²⁷ this value is 1.4.

Previous ultrasonic measurements indicated² that the ultrasonic attenuation of NH₃-I became very high along the dashed curve in Fig. 1. This occurs at 175 K at zero pressure, 188 K at 2.0 kbar, and 202 K at 4.0 kbar. These temperatures are indicated in Fig. 4 by short lines crossing the relevant data curves. Clearly, T_1 and T_{1D} vary smoothly at all temperatures. There is no indication in the proton NMR data of any change in the sample in the region where the ultrasonic attenuation increases.

Deuteron NMR of ND₃-I was studied at only one pressure, 4.0 kbar. The deuteron T_1 is determined by the modulation of the quadrupole interaction by the threefold reorientations. Because the same motion is involved in the proton T_1 mechanism, it is expected that the proton and deuteron T_1 have the same temperature dependences. As shown in Fig. 5, this is the case.

Diffusion can be detected in the quadrupole-broadened deuteron spectrum in two ways. The first method uses quadrupole spin echoes³⁹ generated with the 90_x-t-90_y pulse sequence. The second pulse causes a refocusing to occur at time $2t$, but only for those spins which have remained in the same EFG from time zero to $2t$. Because ND₃-I is orientationally ordered and because molecules in nearest-neighbor sites have different orientations than in the central site, molecules that diffuse change their orientation and hence change the EFG present at the deuteron nuclei. Thus, the echo amplitude will decay as a function of the pulse spacing t :

$$A(t) \propto e^{-2t/\tau_j}. \quad (8)$$

At low temperatures where τ_j is long, the echo envelope is damped by spin-spin interactions. As shown in Fig. 5 as solid triangles, below 195 K the echo-envelope decay-time constant T_2 is essentially independent of temperature. This T_2 does not reflect jump diffusion, but arises only from spin-spin coupling. Above 195 K, T_2 decreases with temperature, due to diffusion. However, the data do not extend over a wide enough temperature interval for proper analysis of the diffusion.

The stimulated echo^{40,41} (spin-alignment echo) has been used to measure slower diffusion. The decay-time constant τ^* is displayed in Fig. 5 as solid squares. At high

temperatures the ND₃-I τ^* data and NH₃-I T_{1D} data are nearly parallel. Given the poorer signal-to-noise ratio available with ND₃-I, we conclude that the two isotopes have the same activation energies for self-diffusion, within 5%. However, the τ^* values are consistently about a factor of 6 longer than the T_{1D} values at the same temperature. Since τ^* should be equal to the diffusion jump time and T_{1D} is, at most, a factor of 2 shorter than τ_j [see Eq. (7) with $p=0$], it appears that diffusion in ND₃-I is at least a factor of 3 slower than in NH₃-I. This is an unexpected isotope effect.

At low temperature, τ^* is found to be about 1.8 times longer than the deuteron T_1 . This is because $\Delta m = \pm 2$

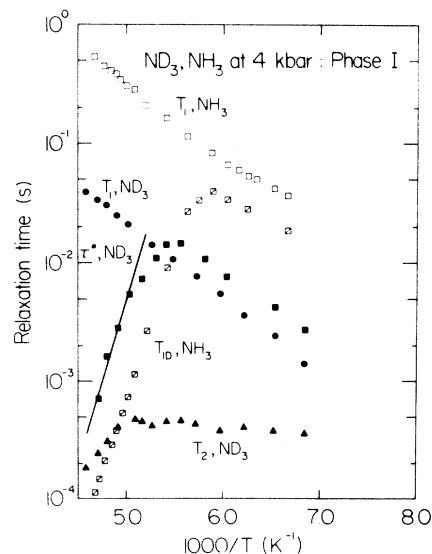


FIG. 5. Proton and deuteron relaxation times from ammonia phase I at 4.0 kbar. The proton (open squares) and deuteron (solid circles) T_1 are both determined by threefold reorientations; note the parallel temperature dependences. The deuteron τ^* data (solid squares) are from spin-alignment (stimulated) echoes. Like the proton T_{1D} data (hatched squares), the τ^* values should equal the mean jump diffusion time τ_j to within a factor near unity. The ND₃ T_2 values (solid triangles) are limited by spin-spin coupling, but they begin to reflect jump diffusion near the melt.

transitions are not effective in destroying spin alignment (Y_{20} order). Spiess has shown⁴⁰ that in the case of fast motions (the threefold reorientations do satisfy $\omega_3 \gg \omega_{\text{NMR}}$), $\tau^*/T_1 = 5/3$. The agreement with the experimental result is quite good.

The deuteron NMR data in Fig. 5 show only smooth behavior near the ultrasonic attenuation onset ($1000/T = 4.95 \text{ K}^{-1}$).

CONCLUSIONS

NMR experiments demonstrate that the high-pressure phase (II) of solid ammonia is a typical rotor ("plastic") crystal. The narrow NMR lines from NH_3 and ND_3 indicate that rapid reorientations and translational diffusion occur in phase II. From the proton T_1 , the diffusion jump time is inferred to be 6×10^{-8} s near the melt with an activation energy of 4400 K ($\pm 20\%$). These values agree via scaling relations with values found in many simple rotor solids. The orientation correlation time is deduced to be 1.0×10^{-12} s from the deuteron T_1 of ND_3 -II. This value is substantially longer (factor of 14) than the inertial limit. However, the value is typical of simple rotor solids.

A small splitting is observed in ND_3 -II, confirming the noncubic (hexagonal) structure of II obtained from neutron diffraction. The quadrupolar deviation from isotropy of the molecular orientation probability is given by $|\langle \frac{3}{2} \cos^2 \theta - \frac{1}{2} \rangle|$ and is only of order 0.005. This suggests a nearly isotropic orientation probability distribution.

In phase I the proton and deuteron T_1 's are determined by the rate of thermally activated threefold reorientations. The pressure dependence of the proton T_1 indicates a

small activation volume (0.1 molar volume), as expected for in-place reorientations. The proton T_{1D} and deuteron spin-alignment data follow the rate of diffusion in ammonia phase I. The temperature dependences indicate a higher jump-rate prefactor (ω_0) than found previously. The value found here in NH_3 -I, $5 \times 10^{17} \text{ s}^{-1}$, is orders of magnitude larger than the Debye frequency but similar to values in other orientationally ordered solids. The activation volume of diffusion, determined from the pressure dependence of T_{1D} , is about 0.78 molar volume; this is reasonable for a vacancy process. An isotope effect upon diffusion occurs in phase I, the diffusion in ND_3 -I being at least 3 times slower than in NH_3 -I at the same temperature.

There is no indication in the phase-I NMR data of any changes that can be associated with the anomalous ultrasound attenuation.

ACKNOWLEDGMENTS

We appreciate several helpful discussions with R. L. Mills, D. H. Liebenberg, and R. Fisch. We gratefully acknowledge the expert advice of W. B. Daniels on high-pressure gas techniques. The work at the College of William and Mary was funded by the Jeffress Memorial Trust Fund; one of us (M.S.C.) was supported in part by the Alfred P. Sloan Foundation. The work at Washington University was funded by the National Science Foundation Low Temperature Physics Program, under grant No. DMR-83-04473. We thank J. R. Brookeman for the loan of the high-pressure helium apparatus. The magnet used in this work was a gift of E. I. duPont de Nemours and Co.

¹Ph. Pruzan, D. H. Liebenberg, and R. L. Mills, *Phys. Rev. Lett.* **48**, 1200 (1982).
²R. L. Mills, D. H. Liebenberg, and Ph. Pruzan, *J. Phys. Chem.* **86**, 5219 (1982).
³R. L. Mills, D. H. Liebenberg, R. LeSar, and Ph. Pruzan, in *High Pressure in Science and Technology*, edited by C. Homan, R. K. MacCrone, and E. Whalley (North-Holland, New York, 1984), Vol. 22, Pt. 2, p. 43.
⁴J. Eckert, R. L. Mills, and S. K. Satija, *J. Chem. Phys.* **81**, 6034 (1984).
⁵R. C. Hanson and M. Jordan, *J. Phys. Chem.* **84**, 1173 (1980).
⁶I. Olovsson and D. H. Templeton, *Acta Crystallogr.* **12**, 832 (1959).
⁷J. W. Reed and P. M. Harris, *J. Chem. Phys.* **35**, 1730 (1961).
⁸J. L. Carolan and T. A. Scott, *J. Magn. Reson.* **2**, 243 (1970).
⁹D. E. O'Reilly, E. M. Peterson, and S. R. Lammert, *J. Chem. Phys.* **52**, 1700 (1970).
¹⁰D. E. O'Reilly and E. M. Peterson, *J. Chem. Phys.* **56**, 5536 (1972).
¹¹T. A. Scott, *Phys. Rep.* **27**, 89 (1976).
¹²R. A. Pethrick, in *The Plastically Crystalline State*, edited by J. N. Sherwood (Wiley, New York, 1979), p. 123.
¹³R. H. Cornish and A. L. Ruoff, *Rev. Sci. Instrum.* **32**, 639 (1961).
¹⁴P. L. Kuhns and M. S. Conradi, *J. Chem. Phys.* **80**, 5851 (1984).

¹⁵N. Boden, in *The Plastically Crystalline State*, Ref. 12, p. 147.
¹⁶J. van Liempt, *Z. Phys.* **96**, 534 (1935).
¹⁷L. V. Dmitrieva and V. V. Moskalev, *Fiz. Tverd. Tela (Leningrad)* **5**, 2230 (1963) [*Sov. Phys.—Solid State* **5**, 1623 (1964)].
¹⁸C. P. Slichter, *Principles of Magnetic Resonance* (Springer, New York, 1980).
¹⁹H. A. Resing and H. C. Torrey, *Phys. Rev.* **131**, 1102 (1963).
²⁰J. G. Powles and M. Rhodes, *Mol. Phys.* **12**, 399 (1967).
²¹A. S. DeReggi, P. C. Canepa, and T. A. Scott, *J. Magn. Reson.* **1**, 144 (1969).
²²M. A. Doverspike and M. S. Conradi, *Phys. Rev. B* **30**, 4905 (1984).
²³F. Li, J. R. Brookeman, A. Rigamonti, and T. A. Scott, *J. Chem. Phys.* **74**, 3120 (1981).
²⁴A. Abragam, *The Principles of Nuclear Magnetism* (Oxford University Press, Oxford, 1983).
²⁵W. A. Steele, in *Advances in Chemical Physics*, Vol. 34, edited by I. Prigogine and S. A. Rice (Wiley, New York, 1976).
²⁶R. Folland, S. M. Ross, and J. H. Strange, *Mol. Phys.* **26**, 27 (1973).
²⁷S. McGuigan, J. H. Strange, and J. M. Chezeau, *Mol. Phys.* **47**, 373 (1982).
²⁸Yu. G. Kriger and B. I. Obmoin, *Fiz. Tverd. Tela (Leningrad)* **20**, 1532 (1978) [*Sov. Phys.—Solid State* **20**, 883 (1978)].
²⁹C. P. Slichter and D. C. Ailion, *Phys. Rev.* **135**, A1099 (1964).

- ³⁰D. C. Ailion, in *Advances in Magnetic Resonance, Vol. 5*, edited by J. S. Waugh (Academic, New York, 1971).
- ³¹D. C. Ailion and P.-P. Ho, *Phys. Rev.* **168**, 662 (1968).
- ³²D. Wolf, *Phys. Rev. B* **10**, 2724 (1974).
- ³³S.-B. Liu and M. S. Conradi, *Phys. Rev. B* **30**, 24 (1984).
- ³⁴S.-B. Liu, M. A. Doverspike, and M. S. Conradi, *J. Chem. Phys.* **81**, 6064 (1984).
- ³⁵K. R. Nary, P. L. Kuhns, and M. S. Conradi, *Phys. Rev. B* **26**, 3370 (1982).
- ³⁶F. Noack, M. Weithase, and J. von Schutz, *Z. Naturforsch.* **30**, 1707 (1975).
- ³⁷T. Gullion and M. S. Conradi, *Phys. Rev. B* (to be published).
- ³⁸R. Overstreet and W. F. Giauque, *J. Am. Chem. Soc.* **59**, 254 (1937).
- ³⁹H. W. Spiess, *Colloid Polym. Sci.* **261**, 193 (1983).
- ⁴⁰H. W. Spiess, *J. Chem. Phys.* **72**, 6755 (1980).
- ⁴¹M. Lausch and H. W. Spiess, *J. Magn. Reson.* **54**, 466 (1983).